

Design and Preparation of Rapid Full Bio-Degradable Plastic Composites Based on Poly(Butylene Succinate)

Yi Xie, Jihai Zhang, Jingying Hu, Aiming Zhang, Tao Zhou 

State Key Laboratory of Polymer Materials Engineering of China, Polymer Research Institute, Sichuan University, Chengdu 610065, China

Rapid full bio-degradable plastic composites based on poly(butylene succinate) (PBS) were successfully designed and prepared. The bio-degradation behavior of the composites was focused on. Results demonstrated that the polymer composites incorporated with starch exhibited a rapid biodegradability. Only after 5 months of biodegradation, the polymer composites with 40 and 50 wt% starch were fully pulverized in the soil. However, mechanical properties of composites were also seriously deteriorated. Theory calculations and scanning electron microscopy confirmed the reason is the poor interface adhesion between PBS and starch. To address this issue, maleic anhydride grafted PBS (PBS-g-MAH) was prepared to use as the polymer matrix. As expected, the good mechanical properties were obtained due to an excellent adhesion in the interface. For instance, the tensile strength was increased from 15.0 to 23.0 MPa, and the impact strength is enhanced from 6.5 kJ/m² to 11.9 kJ/m² when the amount of MAH and dicumyl peroxide were 2 and 0.2 wt%, respectively. In addition, the use of PBS-g-MAH further increased the biodegradation rate of the composites. The PBS-g-MAH/starch (60/40) composites were fully pulverized in soil only after 3 months of biodegradation. Fourier transform infrared spectroscopy (FTIR) also revealed the compatibilizing mechanism between PBS-g-MAH and starch was that MAH reacted with hydroxyl groups in the starch to produce the ester. As an attractive full biodegradable polymer, the low-cost composites proposed here will have wide prospects of application in the near future. *POLYM. COMPOS.*, 39:E609–E619, 2018. © 2018 Society of Plastics Engineers

INTRODUCTION

Nowadays, the environmental problem of “white” pollution is attracting more and more attention by people, and the development and application of biodegradable plastics is one way to solve this issue. Moreover, with the increasing depletion of oil resources, searching environmental-friendly alternatives for petroleum-based materials also gradually becomes a trend, especially in the fields of packaging, health, and agriculture [1–4]. As expected, scientists have developed many bio-degradable plastics, such as poly(lactic acid) [5, 6], polycaprolactone [7], and poly(butylene succinate) (PBS) [8, 9]. Some of them even can be produced from renewable resources [10, 11].

For the biodegradable polymers listed earlier, PBS has been received so much attention in recent years, because not only it has an excellent full biodegradability in nature, but also owns similar mechanical properties with the general plastics such as polyethylene, polypropylene, polystyrene, and so forth [12, 13]. PBS is a white crystalline thermoplastic, which is synthesized *via* the condensation reaction of the glycols 1,4-butanediol and succinic acid or obtained by the fermentation process of crop products containing cellulose, glucose, fructose, and lactose [14]. PBS is also a typical fully biodegradable polymer material, which can be easily metabolized and ultimately broken down into carbon dioxide and water by various natural microorganisms and plant enzymes. However, at present, the price of PBS is still high, and therefore, the application of PBS is greatly limited [15]. Fortunately, the use of other low-cost materials to produce PBS composite is an effective way to reduce the application cost of PBS. For this issue, the starch is a good choice to prepare the PBS composite. This is because the PBS/starch composite still owns a full biodegradability; moreover, the cost of starch is very low.

Another important thing is that the biodegradation rate of neat PBS is not fast enough in a given degradation environment [16, 17]. The starch as a highly water-absorbing substance is expected to accelerate the biodegradation rate of PBS, and this is also the original intention of our work [18, 19]. As is known, the starch is a kind of

Correspondence to: T. Zhou; e-mail: zhoutaopoly@scu.edu.cn

Contract grant sponsor: National Natural Science Foundation of China; contract grant numbers: 51473104 and 51773126; contract grant sponsor: Outstanding Youth Foundation of Sichuan Province; contract grant number: 2017JQ0006; contract grant sponsor: State Key Laboratory of Polymer Materials Engineering; contract grant numbers: sklpme2014-3-06, sklpme2016-3-10.

Additional Supporting Information may be found in the online version of this article.

DOI 10.1002/pc.24783

Published online in Wiley Online Library (wileyonlinelibrary.com).

© 2018 Society of Plastics Engineers

polysaccharide stored in the form of granules in plant cells, which is always produced from natural sources, including wheat, rice, corn, potato, and pea [20]. Judging from the molecular structure, starch is composed of amylose and amylopectin in general. The amylose is a linear polymer of α -1,4-linked glucose units, and amylopectin is a branched polymer of α -1,4-linked chains interlinked with 1,6-linkages glucose units [21]. The presence of glucose units endows the starch with strong intra/intermolecular hydrogen bonds, resulting in non-thermoplastic processability. Thus, the starch is generally used as organic filler in polymer matrix composites. It should be pointed out that PBS is a typical aliphatic polyester, which is a hydrophobic (or semi-hydrophobic) polymer; however, the starch is inherently hydrophilic. Consequently, these two polymers are thermodynamically immiscible, which would result in a poor adhesion between these two components in composites and causes a poor mechanical performance [22]. Scientists have proposed several ways to solve this problem. For example, Suchao-in et al. [18] prepared starch-g-PBS to promote the interfacial adhesion between PBS and starch, and their results showed that the starch-g-PBS is a good compatibilizer. Zeng et al. [9] synthesized reactive PBS with terminal $N=C=O$ groups to obviously enhance the miscibility between starch and PBS. Yin et al. [23] proposed using maleic anhydride grafted PBS (PBS-g-MAH) as an interfacial compatibilizer, and the results demonstrated that the mechanical properties of the PBS/starch blend were greatly increased by adding PBS-g-MAH in PBS/starch blends. The above problem is also inevitable in our work.

In our study, we directly used PBS-g-MAH as the polymer matrix to prepare the PBS/starch composite, and therefore, the composites owning both high performance and rapid biodegradation were obtained. Here, PBS/starch composites and PBS-g-MAH/starch composites were prepared and studied. Our research focused on biodegradation behaviors of the composites. When compared with the neat PBS, the cost of PBS/starch composites is obviously reduced, and the degradation rate is expected to significantly accelerate without the negative impact on mechanical properties.

EXPERIMENTAL

Materials

PBS (HX-B601, melt flow rate = 78.0 g/10 min, $M_w = 1.2 \times 10^5$ g/mol) was obtained from Hexing Chemical Co. Ltd (China). The granular corn starch (food grade, 12% moisture, average particle size = 10 μ m) was purchased from Jianmin Starch Co. Ltd (China). Maleic anhydride and dicumyl peroxide (DCP) were obtained from Kelong Chemical Reagent Factory (China). All solvents used in this study were analytical grade.

Sample Preparation

Preparation of PBS/Starch Composites. PBS and corn starch were firstly dried in the vacuum oven (the vacuum degree = -0.08 MPa) at 70°C for 24 h. Then, PBS and corn starch were mechanically mixed using a high speed mixer. After that, the PBS/starch composites were prepared *via* melting blending by a laboratory twin-screw extruder ($\Phi 20$, aspect ratio = 32:1) at 170°C. Five composites were prepared, and the weight ratios of PBS to starch were 90:10 (10 wt%), 80:20 (20 wt%), 70:30 (30 wt%), 60:40 (40 wt%), and 50:50 (50 wt%), respectively.

Preparation of PBS-g-MAH/Starch Composites. Here, the PBS-g-MAH was first prepared. The MAH and DCP were dissolved with acetone, respectively, and then mixed with PBS. After that, the mixtures were dried in the oven at 60°C to remove the residual acetone. PBS-g-MAH was fabricated *via* the reactive extrusion by a laboratory twin-screw extruder ($\Phi 20$, aspect ratio = 32:1) at 170°C. Ten types of PBS-g-MAH were prepared with the different DCP and MAH amount in the reactive extrusion. For the first group, the amount of DCP was fixed at 0.2 wt%, and that of MAH used was 1, 2, 3, 4, and 5 wt%, respectively. For the second group, the amount of MAH was fixed at 1 wt%, and that of DCP added was 0.1, 0.2, 0.3, 0.4, and 0.5 wt%, respectively. In this work, the meaning of MAH content or DCP content referred to the weight percentage of PBS-g-MAH. For example, MAH content was 1 wt% that referred to 1 wt% of PBS-g-MAH.

The prepared PBS-g-MAH above and corn starch were dried in the vacuum oven (the vacuum degree = -0.08 MPa) at 70°C for 24 h. Then, the prepared PBS-g-MAH was mechanically mixed with corn starch using a high speed mixer. After that, PBS-g-MAH/starch composites were fabricated using a laboratory twin-screw extruder ($\Phi 20$, aspect ratio = 32:1) at 170°C. Ten composites were prepared, and the weight ratio of PBS-g-MAH to starch was all fixed at 60:40 (40 wt%).

Characterization and Testing

Biodegradation in Soil. The biodegradation experiments in soil were performed in a container (diameter = 30 cm; height = 20 cm) filled with soil. The soil was composed of top soil and black garden soil (the weight ratio = 1:1) with pH value of 7 and the moisture content of 50%. After drying and weighting, the composite specimens ($30 \times 10 \times 4$ mm³) were buried into the soil. The biodegradation experiments were carried out for 5 months. Every other month the specimens were dug out from the soil and wiped using the tissue paper. The specimens were further cleaned with running water and dried at 60°C in a vacuum oven (the vacuum degree = -0.08 MPa), and then weighted and photographed.

Water Absorption. Water absorption measurements were carried out using ASTM D570 method at 23°C. The composite specimens ($20 \times 20 \times 1 \text{ mm}^3$) were firstly dried at 60°C in a vacuum oven (the vacuum degree = -0.08 MPa) until a constant weight was obtained, and then immersed in the distilled water. After that, the samples were taken out of the water at a regular interval (24 h) and weighted. The above procedure was repeated until the weight of the samples was constant.

The water absorption of the samples was calculated according to the following Equation:

$$M_t(\%) = (W_w - W_d) / W_d \times 100 \quad (1)$$

where W_d is the weight of the completely dried samples, and W_w is the weight of the corresponding samples after absorbing water.

Mechanical Properties. Tensile strength and Izod impact strength were tested according to ISO 527-1,2 and ISO 180, respectively. The test samples were prepared by injection molding (K-TEC 40, Milacron, USA) operated with a nozzle temperature of 175°C. Tensile test was performed on a universal testing machine (Instron 5567) equipped with a 10 kN electronic load cell and mechanical grips. The crosshead speed was set at 50 mm/min. Izod impact test was performed using a standard impact testing machine (XBJ-0.75/11, XinKe Co., Ltd., China). For each composite, the samples were tested at least five times to obtain the average value.

Scanning Electron Microscopy. The samples of composites were firstly fractured in liquid nitrogen. Then, the scanning electron microscopy (SEM) images of the section morphology were observed using a JSM-5900 LV SEM (JEOL, Japan) at an accelerating voltage of 25 kV. To prevent the electrical discharge, the fractured samples were coated with a thin gold before the SEM observation.

FTIR Spectroscopy. The PBS/starch composite and PBS-g-MAH/starch composite were extracted with chloroform at 80°C for 10 h using Soxhlet extraction to completely remove PBS or PBS-g-MAH without reacting with starch. The dry residue after the extraction was the powder, and then we grounded 5–8 mg of this powder with 250 mg KBr until the powder was uniformly dispersed. The mixed powder was tableted to a disk with the diameter of 1.3 cm and the thickness of 0.8 mm. After that, the FTIR spectra were collected with Nicolet iS10 Fourier transform spectrometer equipped with a deuterated triglycine sulfate detector. The FTIR spectra of the samples were recorded within the region of $4,000 - 400 \text{ cm}^{-1}$ at a resolution of 4 cm^{-1} with 20 scans.

Differential Scanning Calorimetry (DSC). DSC measurements were performed using NETZSCH DSC 204 F1 in nitrogen atmosphere. The samples were firstly heated

from 20 to 160°C at 40°C/min, and then kept at 160°C for 2 min to eliminate the thermal history. After that, the samples were cooled from 160 to 10°C at 10°C/min, and then kept at 10°C for 2 min. Finally, samples were heated from 10 to 160°C at 10°C/min. The sample weight was 7 mg, and the nitrogen flow rate was 25 mL/min. Before DSC measurements, all the samples were dried at 70°C for 24 h in a vacuum oven (the vacuum degree = -0.08 MPa).

Melt Flow Index. The melt flow index was estimated using ASTM D1238 standard. The tests were performed at 170°C with a load of 2.16 kg. For each sample, six tests were carried out to obtain the average value.

The melt flow index of the samples was calculated according to the following Equation:

$$MI = m \times 60 \quad (2)$$

where MI is the melt flow index, and m is the average mass of plastic melt outflowed for every 10 s.

RESULTS AND DISCUSSION

Biodegradation Experiments of PBS/Starch Composites

For the rapidly biodegradable plastic composite, its degradation behavior is the most attention for us. The digital photographs of the PBS and PBS/starch composites after biodegradation in soil for 1, 3, and 5 months are shown in Fig. 1a. It can be observed that the biodegradation rate of neat PBS is very slow, and after 5 months biodegradation in soil, it has no other change in appearance except for some slight variations in color. However, as expected, once incorporated with starch, the PBS/starch composites show an obvious biodegradability. Specifically, with the extension of the biodegradation time, not only the color of the composites is apparently deepened, but also the surface of the composites becomes particularly rough, showing a typical “bio-corrosion” phenomenon. Importantly, the observations from Fig. 1a clearly indicate the acceleration of biodegradation rate of PBS/starch composites with the increase of starch content from 10 to 50 wt%. This is because after 3 months of biodegradation, the PBS/starch composite with 50 wt% starch was fully pulverized in the soil and we couldn't collect at all in our experiments; similarly, after 5 months, the PBS/starch composite with 40 wt% starch was also fully pulverized.

Figure 1b is the residual weight of neat PBS and PBS/starch composites after biodegradation in soil with different months, which can quantitatively describe the biodegradation behavior of composite materials. For neat PBS, its weight is almost no change after 5 months, directly showing no (or slight) biodegradation even after 5 months of soil burying. However, for PBS/starch composites, the weight of the sample is reduced only after 1 month,

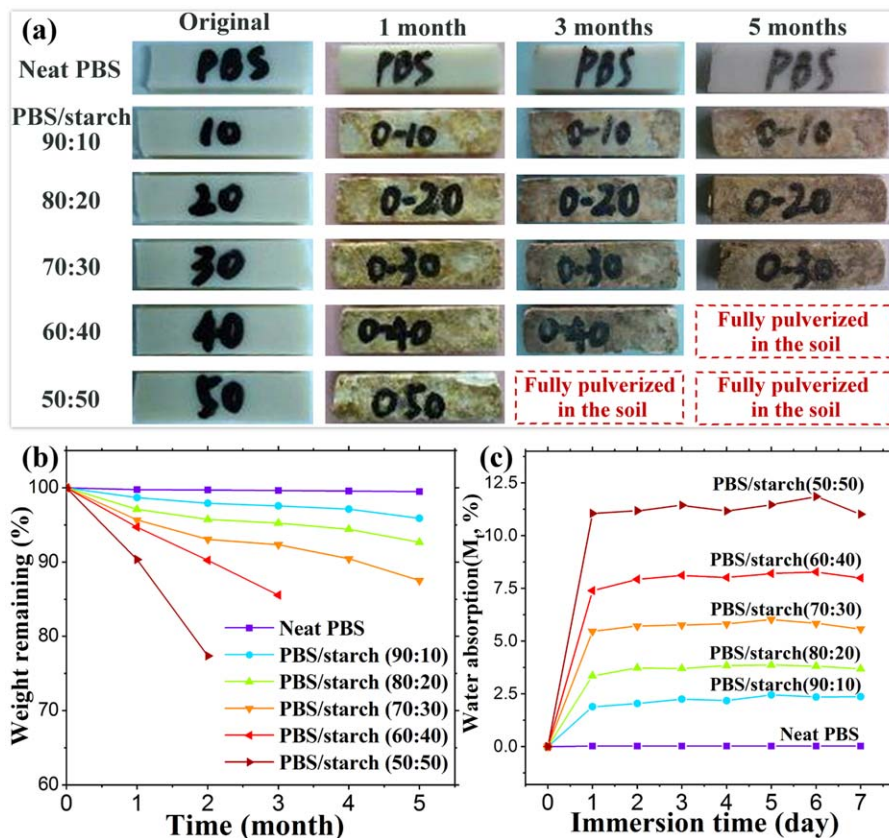


FIG. 1. (a) Digital photographs of neat PBS and PBS/starch composites after biodegradation in soil for 1, 3, and 5 months; (b) residual weight of neat PBS and PBS/starch composites after biodegradation in soil; (c) water absorption of neat PBS and PBS/starch composites with different time.

especially the fact that about 10% weight loss of the composite with 50 wt% starch is observed only after 1 month. After 2 months of biodegradation, the residual weight of neat PBS and PBS/starch composites with the starch content of 10, 20, 30, 40, 50 wt% are 99.7, 97.9, 95.7, 93.1, 90.2, and 77.4%, respectively. Moreover, the weight loss of PBS/starch composites is further increased with the extension of the biodegradation time from 3 to 5 months. That is to say, the “bio-corrosion” rate of PBS/starch composites is much higher than that of neat PBS, and the more starch gives a faster biodegradability.

Here, as shown in Fig. 1c, the water absorption behavior of neat PBS and PBS/starch composites with different time was also measured. The neat PBS exhibits very low water absorption, and the water absorption of neat PBS is only 0.02 wt% after 7 days. The water absorption of PBS/starch composites is significantly increased, and the saturation state is reached only after 1 day. Seven days later, the water absorption of PBS/starch composites with the starch content of 10, 20, 30, 40, 50 wt% are 2.36, 3.68, 5.58, 7.99, 11.01% respectively. It can be observed that the results of water absorption are directly correlated with those of biodegradation rate. That is to say, compared with neat PBS, the acceleration of the “bio-corrosion” rate of PBS/starch composites is probably caused by the high water absorption

of starch. This is because water molecules can form hydrogen bonds with hydroxyl groups in starch, and the increase of water absorption greatly promotes the growth of bacteria in composites’ matrix, thereby improving the biodegradation rate.

Mechanical Properties of PBS/Starch Composites

Mechanical properties of composites are needed to focus on. Figure 2a and b are the tensile strength and impact strength of neat PBS and PBS/starch composites with different starch content. Disappointingly, a rapid decline was observed with the increase of the starch content. Actually, the neat PBS exhibited good mechanical properties with tensile strength of 30.7 MPa and a high-impact strength (it was unbroken in our impact testing). However, with the increase of starch content from 10 to 50 wt%, both the tensile strength and impact strength were decreased significantly. Especially, the tensile strength of the composite is reduced to 11.63 MPa when the starch content is 50 wt%, only 37.9% of neat PBS. And, its impact strength is also rapidly decreased to 5.1 kJ/m². This indicates that the application of PBS/starch composites is difficult due to the poor mechanical property, even if the composites have a rapid biodegradability.

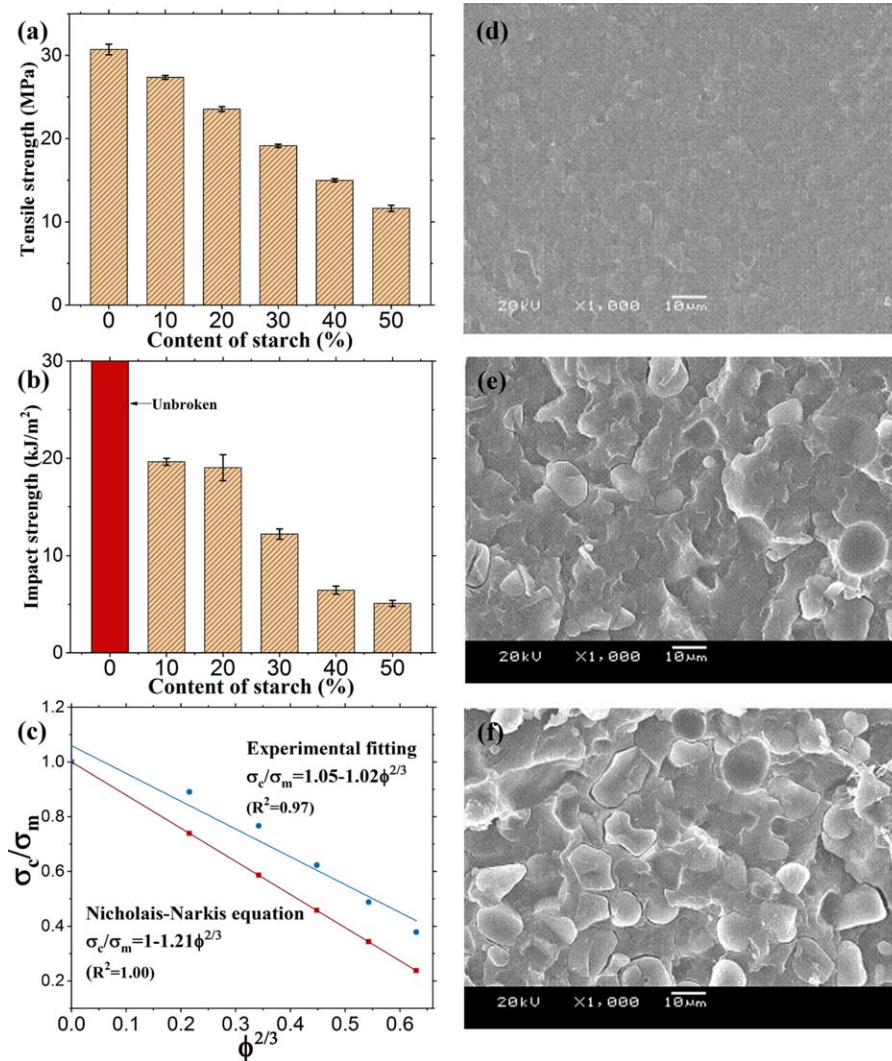


FIG. 2. (a) Tensile strength of PBS/starch composites with different starch content; (b) impact strength of PBS/starch composites with different starch content; (c) prediction (red line) of tensile strength for incompatible PBS/starch composites according to Nicholais-Narkis Equation and the linear fitting of experimental tensile strength (blue line) of PBS/starch composites; (d) SEM image of the cross-section of neat PBS; (e) SEM image of the cross-section of PBS/starch composites (80:20); (f) SEM image of the cross-section of PBS/starch composites (60:40).

To explain the reason for the low mechanical properties of PBS/starch composites, some calculations and fitting were performed according to the experimental tensile strength. In general, the Nicholais-Narkis model can be used to describe and predict the tensile properties of polymer composites. This model is based on the assumption that the decrease of tensile strength comes from the decrease in the effective cross-sectional area of the matrix material caused by spherical filler particles.

Nicholais-Narkis model is represented by the following Equation:

$$\sigma_c = \sigma_m(1 - a\phi_f^b) \quad (3)$$

where ϕ_f is the volume fraction of filler in the composite, and σ_m is the tensile strength of polymer matrix. The σ_c represents the tensile strength of the composites with

different volume fraction. The a and b are parameters of the filler-matrix interaction and the geometry of filler, respectively.

It usually means a relatively good adhesion between the spherical filler and polymer matrix when the value of a is < 1.21 . If there is no adhesion between the matrix material and the filler in the composites, the Equation becomes:

$$\sigma_c = \sigma_m(1 - 1.21\phi_f^{2/3}) \quad (4)$$

Figure 2c shows the prediction (red line) of tensile strength for PBS/starch composites according to the Nicholais-Narkis Equation and the linear fitting (blue line) of experimental tensile strength (blue points) from Fig. 2a. It can be observed that the experimental tensile strength achieves a successful fitting, which indicates

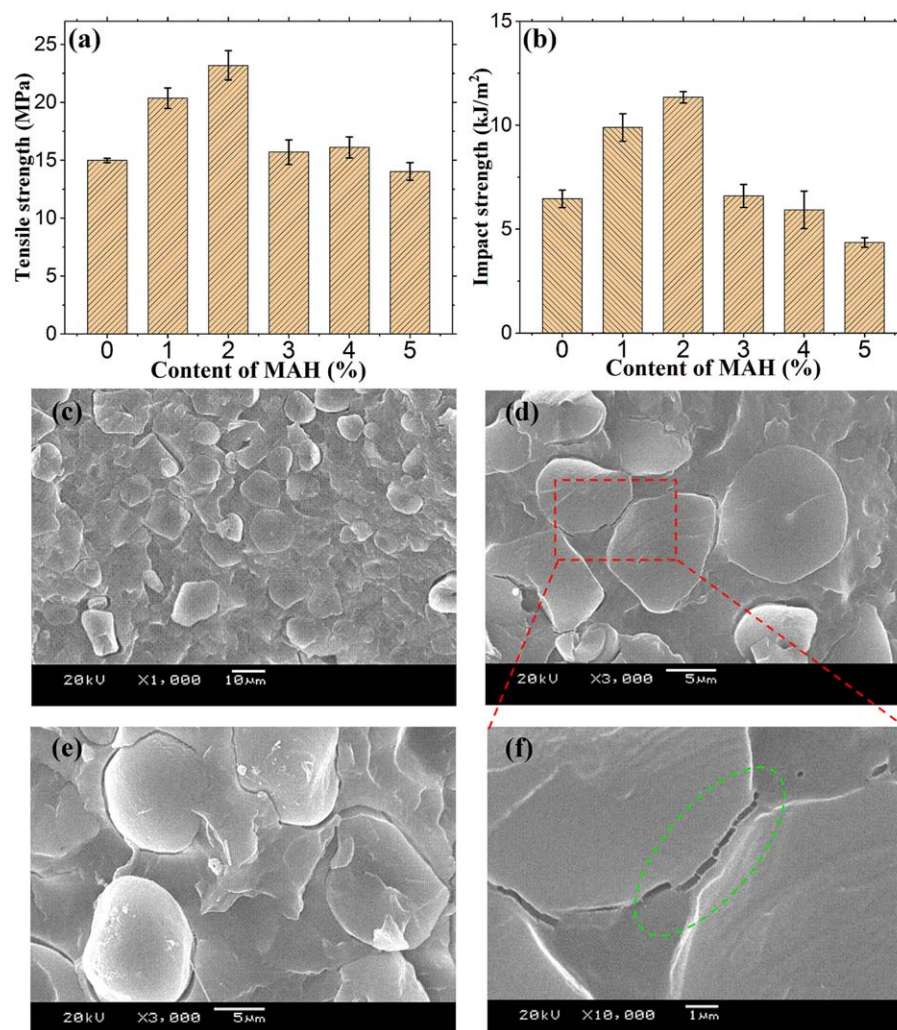


FIG. 3. (a) Tensile strength of PBS-g-MAH/starch (60/40) with different content of MAH; (b) impact strength of PBS-g-MAH/starch (60/40) with different content of MAH; (c) SEM image ($\times 1,000$) of the cross section of PBS-g-MAH/starch (60/40, MAH: 2.0 wt%); (d) SEM image ($\times 3,000$) of the cross section of PBS-g-MAH/starch (60/40, MAH: 2.0 wt%); (e) SEM image ($\times 3,000$) of the cross section of PBS/starch (60/40, MAH: 0 wt%); (f) the enlarged SEM image ($\times 10,000$) of (d).

Nicholais-Narkis model is suitable for PBS/starch composites. The fitting results show that the slope of the fitted line is -1.05 , which is slightly larger than that of the standard Nicholais-Narkis model (-1.21). According to the literature [24], this clearly reveals there still exists some weak adhesion between PBS and starch, namely, a poor interfacial adhesion. As mentioned in the introduction, PBS is a typical a hydrophobic (or semi-hydrophobic) polymer; however, the starch is hydrophilic. Thus, the poor interfacial adhesion between PBS and starch results in a significant decrease of mechanical properties, because the interfacial layer is unable to transfer the stress. The results of fitting give a perfect explanation of this statement. The weak adhesion between starch and PBS is possibly due to hydrogen bonds between the hydroxyl groups of starch and the ester groups of PBS. But this interaction is too weak to prevent the

deterioration of the mechanical properties. Yew et al and Ke et al also had a similar finding [25, 26].

Figure 2d is the SEM image of the cross-section of neat PBS. Figure 2e and f are SEM images of the cross-section of PBS/starch composites with the starch content of 20 wt% (80:20) and 40 wt% (60:40). It can be observed that after the composites fractured, most of the starch particles are directly peeled off from the PBS matrix, leaving only the pits. Besides, those starch particles that are not peeled are simply embedded in the PBS matrix, and the gap between starch particles and PBS matrix can be easily observed. Both these two phenomena also indicate the poor compatibility between starch and PBS. Therefore, if we want to design and prepare PBS/starch composites with both rapid biodegradability and good mechanical performance, the interfacial modification to improve the compatibility is necessary. DSC measurements of neat PBS and

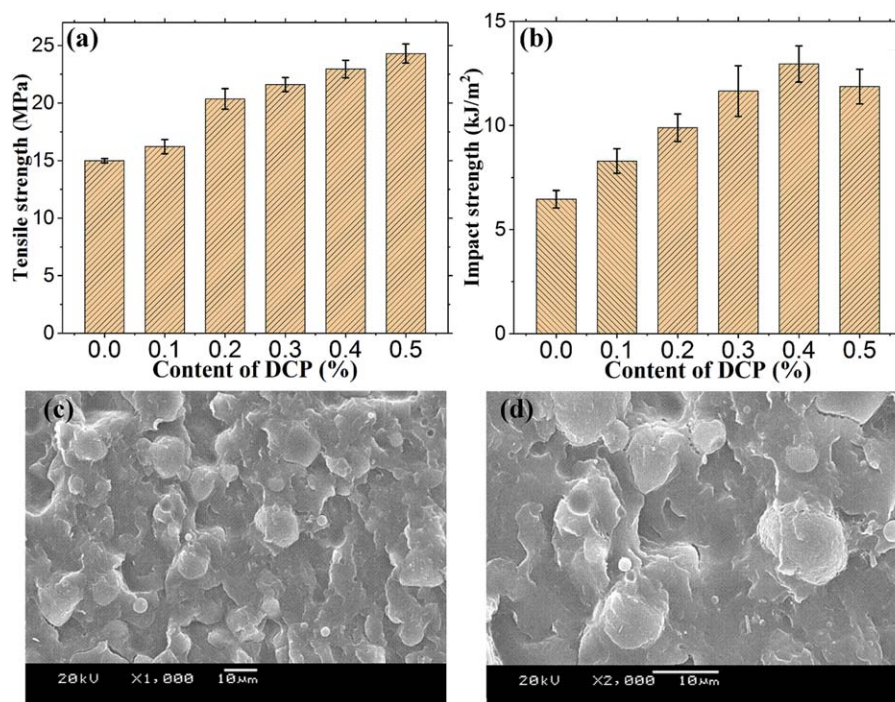


FIG. 4. (a) Tensile strength of PBS-g-MAH/starch (60/40) with different content of DCP; (b) impact strength of PBS-g-MAH/starch (60/40) with different content of DCP; (c) SEM image ($\times 10,000$) of the cross section of PBS-g-MAH/starch (60/40, DCP: 0.3 wt%); (d) SEM image ($\times 2,000$) of the cross section of PBS-g-MAH/starch (60/40, DCP: 0.3 wt%).

PBS/starch composites were also carried out and provided in Supporting Information Fig. S1. For neat PBS, the cold crystallization peak appears at 98°C , and the main melting point is determined at 115°C . With the increase of the starch content, the main melting point of composites fluctuates within $114\text{--}115^{\circ}\text{C}$, which has no change compared with neat PBS. However, the cold crystallization peak moves to 101°C when the content of starch is ≥ 30 wt%.

PBS-g-MAH/Starch Composites

To enhance the compatibility of the two components in the composites, PBS-g-MAH was prepared in our study. Here, PBS-g-MAH was used as the matrix polymer material, other than a compatibilizer reported by other literatures [23]. A series of PBS-g-MAH with the different amount of MAH (grafted monomer) and DCP (free radical initiator) was firstly fabricated *via* the reactive extrusion, and then PBS-g-MAH/starch composites were prepared using a laboratory twin-screw extruder. Considering the cost advantage and a faster biodegradation rate, PBS-g-MAH/starch composites with 40 wt% starch (60:40) was our research object.

Improvement of Mechanical Properties. Two groups of experiments were carried out. In the first group, the amount of DCP was fixed at 0.2 wt%, and that of MAH was changed from 1 to 5 wt%. In the second group, the

amount of MAH was fixed at 1 wt%, and that of DCP used was 0.1, 0.2, 0.3, 0.4, and 0.5 wt%, respectively.

Figure 3a and b illustrate the tensile strength and impact strength of PBS-g-MAH/starch (60/40) composites with different content of MAH. It can be seen that the tensile strength and impact strength of the composites are obviously improved when the amount of MAH is 1 and 2 wt%. The tensile strength is increased from 15.0 to 23.2 MPa, and the impact strength is enhanced from 6.5 to 11.3 kJ/m^2 . However, a sudden decrease is observed for both tensile strength and impact strength when the amount of MAH is ≥ 3 wt%. We think that the hydrolysis degradation of PBS caused by the excessive acidic MAH is one of the possible reasons. The evidence can be obtained from Supporting Information Fig. S2, which shows the melting index of PBS-g-MAH/starch (60/40) with different content of MAH. The melting index is rapidly increased from 27.4 to 160.5 g/10 min when MAH is changed from 1 to 5 wt%, which clearly reveals the hydrolysis degradation of PBS resin caused by MAH.

Figure 3c and d show SEM images of the cross section of PBS-g-MAH/starch (60/40) with 2 wt% MAH, and the magnifications are $\times 1,000$ and $\times 3,000$, respectively. After being fractured, none of the starch particles are peeled off from the PBS matrix, and a good adhesion can be observed in the interface between PBS and starch; this is because each starch particle is directly destroyed along the fracture surface. Figure 3f is the enlarged image of the red rectangle in Fig. 3d, and the interface adhesive

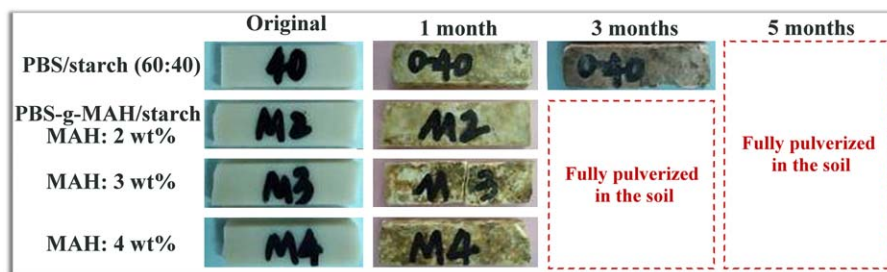


FIG. 5. Digital photographs of PBS/starch composites (60:40) and PBS-g-MAH/starch (60:40) with different dosage of MAH (MAH: 2, 3, and 4 wt%) after biodegradation in soil for 1, 3, and 5 months.

effect can also be seen obviously. Figure 3e is the SEM image of the cross-section of PBS/starch (60/40). In contrast, most of the starch particles in Fig. 3e still exist in the spherical state, and the adhesion in the interface is weak.

DSC curves of PBS/starch (60/40) and PBS-g-MAH/starch (60/40) composites with the different content of MAH are shown in Supporting Information Fig. S3. For the PBS/starch (60/40) composite, the cold crystallization peak is observed at 100°C, and the main melting point appears at 114°C. After using PBS-g-MAH instead of PBS, the main melting point (114–115°C) and the cold crystallization peak (99–101°C) of composites has no obvious variation.

The tensile strength and impact strength of PBS-g-MAH/starch (60/40) composites with different content of DCP are also tested and showed in Fig. 4a and b. The steady increase of tensile strength from 15.0 MPa to 24.3 MPa is observed when the DCP content is changed from 0 to 0.5 wt%. Also, the impact strength of composites has a similar trend, which is enhanced from 6.5 to 13.0 kJ/m² when DCP is increased from 0 wt% to 0.4 wt%, except for a slight decrease (to 11.9 kJ/m²) after using 0.5 wt% DCP. Figure 4c and d are SEM images of the cross section of PBS-g-MAH/starch (60/40) with 0.3 wt% DCP, and their magnifications are $\times 1,000$ and $\times 2,000$, respectively. It can be seen that all the starch particles are almost wrapped by PBS resin, which is different from Fig. 3c and d. This phenomenon reveals that a higher DCP content further improves the adhesion between PBS and starch, and therefore, the steady increase of mechanical properties is observed. However, another fact cannot be ignored. As is known, DCP can cause the crosslinking of most polymers in the process of reaction extrusion [27, 28]. Thus, the increase of mechanical properties is partly attributed to the crosslinking of PBS caused by DCP. The melting index of PBS-g-MAH/starch (60/40) with different content of DCP is provided in Supporting Information Fig. S4. It can be observed that the melting index of composites is rapidly declined from 106.7 to 26.6 g/10 min when DCP is increased from 0.1 to 0.5 wt%, clearly indicating the

DCP crosslinking effect on PBS. We still provide DSC curves of PBS-g-MAH/starch (60/40) composites with the different content of DCP in Supporting Information Fig. S5, and a similar phenomenon with Supporting Information Fig. S3 is observed.

Biodegradation Experiments of PBS-g-MAH/Starch Composites.

As discussed earlier, the mechanical performance of PBS-g-MAH/starch (60/40) is significantly improved than that of PBS/starch (60/40). So, the biodegradability of PBS-g-MAH/starch composite is the focus of our concern. Figure 5 is digital photographs of the PBS/starch (60/40) and PBS-g-MAH/starch (60/40) composites with different dosage of MAH (MAH: 2, 3, and 4 wt%) after biodegradation in soil for 1, 3, and 5 months. The results show the rapid biodegradation rate of both PBS/starch (60/40) and PBS-g-MAH/starch (60/40), and after 5 months all the composites are completely pulverized in the soil. It is worth noting that the biodegradation rate of PBS-g-MAH/starch (60/40) composites is faster than that of PBS/starch, because they are fully pulverized only after 3 months; however, PBS/starch takes 5 months.

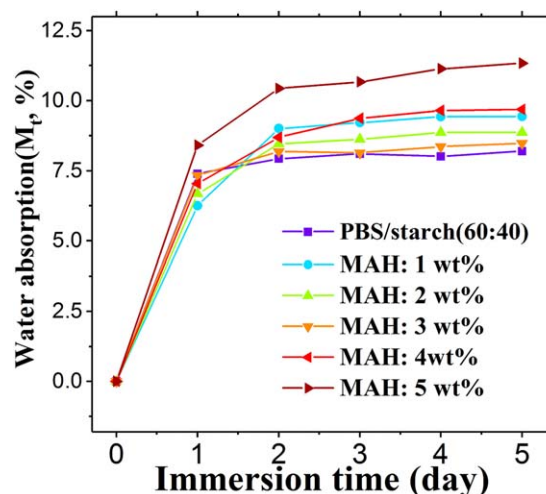


FIG. 6. Water absorption of PBS/starch (60:40) and PBS-g-MAH/starch (60/40) composites with different dosage of MAH (MAH: 1, 2, 3, 4, and 5 wt%) and the different time.

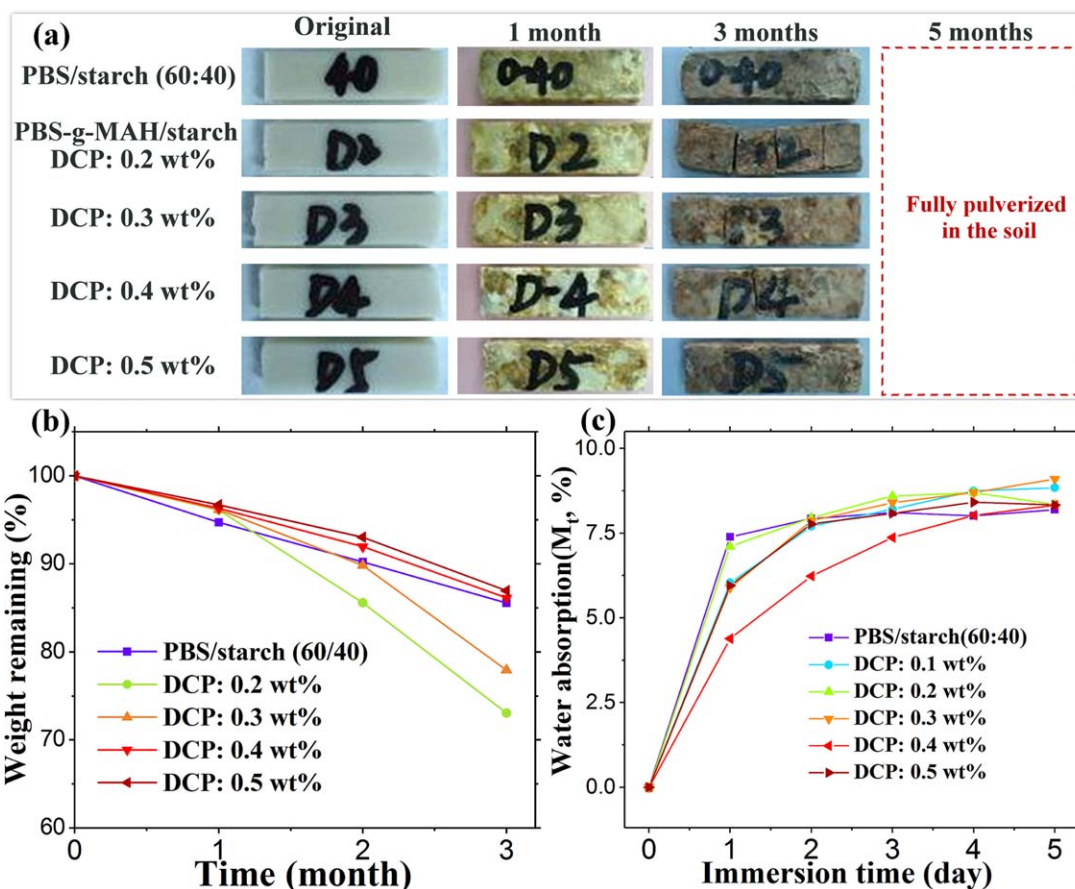


FIG. 7. (a) Digital photographs of PBS/starch composites (60:40) and PBS-g-MAH/starch (60:40) with different dosage of DCP (DCP: 0.2, 0.3, 0.4, and 0.5 wt%) after biodegradation in soil for 1, 3, and 5 months; (B) residual weight of PBS/starch composites (60:40) and PBS-g-MAH/starch (60:40) with different dosage of DCP after biodegradation in soil; (c) water absorption of PBS/starch composites (60:40) and PBS-g-MAH/starch (60:40) with the different time.

Figure 6 is the water absorption of the corresponding PBS/starch (60/40) and PBS-g-MAH/starch (60/40) composites with the different time. When compared with PBS/starch, the results indicate a small increase of the water absorption of PBS-g-MAH/starch (60/40), and the saturation state is reached after 2 days. Five days later, the water absorption of PBS-g-MAH/starch (60/40) composites with the MAH content of 1, 2, 3, 4, and 5 wt% are 9.4, 8.9, 8.5, 9.7, and 11.3%, respectively. And, the water absorption of PBS/starch (60/40) composite is 8.2%, which is smaller than those of PBS-g-MAH/starch (60/40) composites. This indicates that the introduction of MAH further enhances the water-absorbing capacity of composites, leading to a faster biodegradation rate. Also note that, as mentioned in the previous section, the hydrolytic degradation of PBS resin was observed, which was one of the important factors that accelerated the biodegradation of composites.

The digital photographs of the PBS/starch (60/40) and PBS-g-MAH/starch (60/40) composites with different DCP content are shown in Fig. 7a. For PBS-g-MAH/starch composites, the amount of MAH used was fixed at 1 wt%. It can be observed that the PBS/starch (60/40)

and PBS-g-MAH/starch (60/40) composites were fully pulverized in the soil after 5 months of biodegradation. The biodegradation rate of PBS-g-MAH/starch (60/40) composites is almost the same as that of the PBS/starch composite, which is different from Fig. 5. After 3 months, the “bio-corrosion” degree of PBS-g-MAH/starch (60/40) composites with 0.2 and 0.3 wt% DCP seems to be more serious than that of composites with 0.4 and 0.5 wt% DCP.

Figure 7b is the corresponding residual weight of the PBS/starch (60/40) and PBS-g-MAH/starch (60/40) composites with different DCP content after biodegradation in soil with different months. The biodegradation levels of all the composites are increased with the extension of time. After 3 months of biodegradation, the residual weight of PBS-g-MAH/starch (60/40) composites with the DCP content of 0.2, 0.3, 0.4, and 0.5 wt% are 73.1, 78.0, 86.1, and 87.0%, respectively, and the residual weight of PBS/starch (60/40) is 85.5%. That is to say, the biodegradation level of PBS-g-MAH/starch (60/40) composites with 0.4 and 0.5 wt% DCP is close to that of the PBS/starch (60/40) composite. However, the biodegradation level of PBS-g-MAH/starch

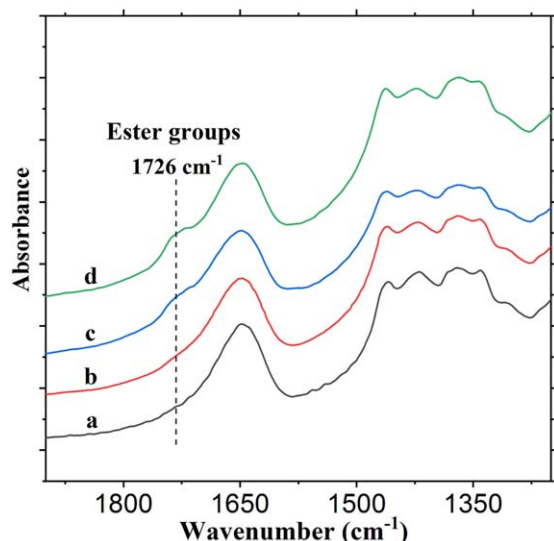


FIG. 8. FTIR spectra of the residual compound of the PBS/starch composite (60/40) and PBS-g-MAH/starch composites (60/40) after soxhlet extraction at 80°C for 10 h using chloroform to completely remove PBS or PBS-g-MAH without reacting with starch. (a) Neat starch; (b) PBS/starch (60/40); (c) PBS-g-MAH/starch (60/40) with 2 wt% MAH; (d) PBS-g-MAH/starch (60/40) with 0.3 wt% DCP.

(60/40) composites with 0.2 and 0.3 wt% DCP is obviously higher. This result can also be observed from Fig. 7b, which shows that the biodegradation of PBS-g-MAH/starch (60/40) composites becomes slow when the DCP content is above 0.4 wt%. As discussed in the previous section, DCP has a significant crosslinking effect on PBS resin, which is the main reason for above phenomenon when a higher amount of DCP is used. Figure 7c is the water absorption of PBS/starch (60/40) and PBS-g-MAH/starch (60/40) composites with the different time. Five days later, the water absorption of PBS/starch (60/40) composite is 8.2%, and the water absorption of PBS-g-MAH/starch (60/40) composites with the DCP content of 0.1, 0.2, 0.3, 0.4, and 0.5 wt% are 8.8, 8.4, 9.1, 8.3, and 8.3%, respectively. This is to say, both PBS/starch (60/40) and PBS-g-MAH/starch (60/40) composites show a similar water absorption here.

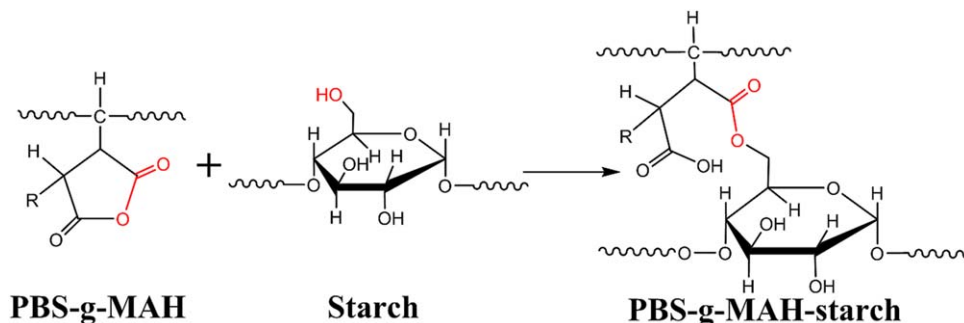
Compatibilizing Mechanism in PBS-g-MAH/Starch Composites. After using PBS-g-MAH instead of PBS, the mechanical properties of composites have been significantly improved; moreover, its biodegradation rate also has a further acceleration. The composite based on PBS owning both good performance and rapid biodegradation has been successfully designed and prepared. However, the compatibilizing mechanism between PBS-g-MAH and starch in composites is still unclear. Here, the FTIR spectroscopy was employed to figure out this issue.

Figure 8 illustrates FTIR spectra of the residues of the PBS/starch composite (60/40) and PBS-g-MAH/starch composites (60/40) after soxhlet extraction at 80°C for 10 h using chloroform to completely remove PBS or PBS-g-MAH without reacting with the starch. For the samples of PBS-g-MAH/Starch (60/40) with 2 wt% MAH and PBS-g-MAH/starch (60/40) with 0.3 wt% DCP, a new peak appears at $1,726\text{ cm}^{-1}$. According to literature [29, 30], this peak at $1,726\text{ cm}^{-1}$ is assigned to the stretching vibration of ester groups. As is known [31–34], MAH in PBS-g-MAH is a typical reactive group, and the compatibilization between PBS-g-MAH and starch is certainly through the chemical reaction between these two components. FTIR spectra in Fig. 8 clearly indicate the generation of ester groups after the compatibilization reaction. Therefore, the probable compatibilizing mechanism between PBS-g-MAH and starch is that MAH reacts with hydroxyl groups in the starch to produce the ester, which is illustrated in Scheme 1.

CONCLUSIONS

This study successfully designed and prepared a rapid full bio-degradable plastic composite based on PBS. The bio-degradation behavior of the composites was the most attention for us, and we started from the interface adhesion to solve the problem of low mechanical properties of the composites.

The results demonstrated that the polymer composites incorporated with starch exhibited a rapid biodegradability. Only after 5 months of biodegradation, the polymer composites with 40 and 50 wt% starch were fully pulverized in the soil. By comparison, it almost has no change



SCH. 1. Reactive compatibilizing mechanism between PBS-g-MAH and starch in composites to improve the interfacial adhesion.

in appearance of neat PBS except for some slight variations in color. However, mechanical properties of composites were significantly deteriorated after incorporating with starch, which is attributed to the poor interface adhesion between PBS and starch, also revealed by theory calculations and SEM. To figure out this problem, PBS-g-MAH was prepared and directly used as the polymer matrix (instead of PBS) to improve the compatibility. The results showed this strategy was effective. For example, the tensile strength was increased from 15.0 to 23.0 MPa, and the impact strength is enhanced from 6.5 to 11.9 kJ/m² when the amount of MAH and DCP were 2 and 0.2 wt%, respectively. SEM images confirmed a good adhesion in the interface between PBS-g-MAH and starch. It was noted that the use of PBS-g-MAH further increased the biodegradation rate of the composites due to the hydrolysis degradation of PBS resin caused by MAH. The PBS-g-MAH/starch (60/40) composite was fully pulverized in soil only after 3 months of biodegradation. In this work, considering both of rapid biodegradation and mechanical performance, the optimal dosages of MAH and DCP were 1.0–2.0 and 0.2–0.3 wt%, respectively. In addition, FTIR spectroscopy confirmed the compatibilizing mechanism between PBS-g-MAH and starch, which MAH reacts with hydroxyl groups in the starch to produce the ester.

Our study also provided a guideline for preparing a rapid full biodegradable plastic composite based on PBS. As an attractive full biodegradable polymer, the low-cost composites proposed here will have wide prospects of application in the near future.

REFERENCES

1. A.-C. Albertsson, I. K. Varma, *Aliphatic Polyesters: Synthesis, Properties and Application*, Springer: Berlin (2002).
2. A.K. Mohanty, M. Misra, and G. Hinrichsen, *Macromol. Mater. Eng.*, **276–277**, 1 (2000).
3. M. Vert, *Biomacromolecules*, **6**, 538 (2005).
4. M. Okada, *Prog. Polym. Sci.*, **27**, 87 (2002).
5. L. Chen, X. Qiu, Z. Xie, Z. Hong, J. Sun, X. Chen, and X. Jing, *Carbohydr. Polym.*, **65**, 75 (2006).
6. Z. Xiong, Y. Yang, J. Feng, X. Zhang, C. Zhang, Z. Tang, and J. Zhu, *Carbohydr. Polym.*, **92**, 810 (2013).
7. P. Sarazin, G. Li, W.J. Orts, and B.D. Favis, *Polymer*, **49**, 599 (2008).
8. T. Ohkita, and S.-H. Lee, *J. Appl. Polym. Sci.*, **97**, 1107 (2005).
9. J.-B. Zeng, L. Jiao, Y.-D. Li, M. Srinivasan, T. Li, and Y.-Z. Wang, *Carbohydr. Polym.*, **83**, 762 (2011).
10. S.-H. Lee, and S. Wang, *Compos. A*, **37**, 80 (2006).
11. K. Oksman, M. Skrifvars, and J.F. Selin, *Compos. Sci. Technol.*, **63**, 1317 (2003).
12. C. Ba, J. Yang, Q. Hao, X. Liu, and A. Cao, *Biomacromolecules*, **4**, 1827 (2003).
13. Y.-D. Li, J.-B. Zeng, X.-L. Wang, K.-K. Yang, and Y.-Z. Wang, *Biomacromolecules*, **9**, 3157 (2008).
14. T. Fujimaki, *Polym. Degrad. Stab.*, **59**, 209 (1998).
15. F. Li, X. Xu, Q. Li, Y. Li, H. Zhang, J. Yu, and A. Cao, *Polym. Degrad. Stab.*, **91**, 1685 (2006).
16. J.-H. Zhao, X.-Q. Wang, J. Zeng, G. Yang, F.-H. Shi, and Q. Yan, *J. Appl. Polym. Sci.*, **97**, 2273 (2005).
17. H.S. Cho, H.S. Moon, M. Kim, K. Nam, and J.Y. Kim, *Waste Manage.*, **31**, 475 (2011).
18. K. Suchao-in, P. Koombhongse, and S. Chirachanchai, *Carbohydr. Polym.*, **102**, 95 (2014).
19. Y. Nabar, J.M. Raquez, P. Dubois, and R. Narayan, *Biomacromolecules*, **6**, 807 (2005).
20. A.A. Karim, A.P.-L. Tie, D.M.A. Manan, and I.S.M. Zaidul, *Compr. Rev. Food. Sci. Food Saf.*, **7**, 215 (2008).
21. S.H. Brown, and R.M. Kelly, *Appl. Environ. Microbio.*, **59**, 2614 (1993).
22. L. Yu, K. Dean, and L. Li, *Prog. Polym. Sci.*, **31**, 576 (2006).
23. Q. Yin, F. Chen, H. Zhang, and C. Liu, *Plast. Rubber. Compos.*, **44**, 362 (2015).
24. H.-M. Park, S.-R. Lee, S.R. Chowdhury, T.-K. Kang, H.-K. Kim, S.-H. Park, and C.-S. Ha, *J. Appl. Polym. Sci.*, **86**, 2907 (2002).
25. G.H. Yew, A.M. Mohd Yusof, Z.A. Mohd Ishak, and U.S. Ishaku, *Polym. Degrad. Stab.*, **90**, 488 (2005).
26. T. Ke, and X. Sun, *Cereal. Chem.*, **77**, 761 (2000).
27. Z. Wang, C.-M. Chan, S.H. Zhu, and J. Shen, *Polymer*, **39**, 6801 (1998).
28. S.W. Hwang, S.B. Lee, C.K. Lee, J.Y. Lee, J.K. Shim, S.E.M. Selke, H. Soto-Valdez, L. Matuana, M. Rubino, and R. Auras, *Polym. Test.*, **31**, 333 (2012).
29. E. Nbedryk, S. Andrianambintsoa, W. Mäntele, J. Breton, *FTIR Spectroscopic Investigations of the Intermediary Electron Acceptor Photoreduction in Purple Photosynthetic Bacteria and Green Plants*, Springer, Boston (1988).
30. P. Luo, H. Niu, G. Zheng, X. Bai, M. Zhang, and W. Wang, *Spectrochim. Acta A*, **74**, 936 (2009).
31. H. Ma, Z. Xu, L. Tong, A. Gu, and Z. Fang, *Polym. Degrad. Stab.*, **91**, 2951 (2006).
32. F. Wang, R.Y. Hong, W.G. Feng, D. Badami, and K. Zeng, *Mater. Lett.*, **125**, 48 (2014).
33. X. Zhang, Y. Chen, Y. Zhang, Z. Peng, Y. Zhang, and W. Zhou, *J. Appl. Polym. Sci.*, **81**, 831 (2001).
34. F. Wang, Y. Zhang, B.B. Zhang, R.Y. Hong, M.R. Kumar, and C.R. Xie, *Compos. B*, **83**, 66 (2015).